Astron. Astrophys. 350, 49–55 (1999)

ASTRONOMY AND ASTROPHYSICS

ISO observations of globular clusters

M.E.L. Hopwood[1], **S.P.S. Eyres**[1,2], **A. Evans**[1], **A. Penny**[3], **and M. Odenkirchen**[4]

[1] Department of Physics, Keele University, Keele, Staffordshire, ST5 5BG, UK (meh@astro.keele.ac.uk)
[2] Astrophysics Research Institute, Twelve Quays House, Egerton Wharf, Birkenhead, L41 1LD, UK (spe@astro.livjm.ac.uk)
[3] Rutherford Appleton Laboratory, Chilton, Didcot, Oxon, OX11 0QX, UK (ajp@astro1.bnsc.rl.ac.uk)
[4] Observatoire de Bordeaux, CNRS/INSU, B.P. 89, F-33270 Floirac, France (odenkirchen@observ.u-bordeaux.fr)

Received 9 March 1999 / Accepted 5 August 1999

Abstract. We report ISO observations of globular clusters, from which we derive new upper limits on the masses of dust therein. Our observations do not confirm the claimed detection of dust in 47 Tuc by Gillett et al. (1988) and our limits generally support previous conclusions that globular clusters are deficient in intra-cluster dust grains. We find that sputtering of dust grains by halo gas is not the mechanism responsible for the removal of such matter, at least in three of the observed clusters. Some other mechanism is therefore at work to remove any dust from the cluster on a short timescale, or the formation of dust within a cluster is inhibited. Our results are consistent with the view that metallicity is the most likely factor concerning the latter point.

Key words: ISM: general – stars: Population II – Galaxy: globular clusters: general – infrared: ISM: continuum

1. Introduction

When a globular cluster (GC) passes through the plane of the Galaxy any interstellar material it contains will be removed tidally and by ram pressure. Typically this will have occured some 10^7....10^8 years ago. Subsequently, the interstellar medium (ISM) of the GC should be replenished with material since a fraction of the stars within the cluster will have progressed to a post-main-sequence evolutionary stage, during which they eject matter into the intra-cluster medium. If each star loses about $0.3\,M_\odot$ during post-main-sequence evolution (Bergbusch & VandenBerg 1992; Richer et al. 1995) we would expect some $0.1...1.0\,M_\odot$ of dust to be present in the cluster.

Despite this, previous observations show that GCs are seriously lacking in intra-cluster material. For example, the only two claimed detections of dust in GCs have been well below expected levels (Gillett et al. 1988; Hopwood et al. 1998; hereafter HEPE and references therein). Observations by Penny et al. (1997), Origlia et al. (1996) and Knapp et al. (1995) also strongly support the hypothesis that some mechanism(s) within the cluster is at work to strip the matter out as it is injected.

We have used the Infrared Space Observatory (ISO) to search for intra-cluster dust in GCs. ISO's better spatial resolution and superior sensitivity (in comparison to its predecessor IRAS and ground-based telescopes) is expected to improve on previous results.

Send offprint requests to: M.E.L. Hopwood

2. Choice of targets

Suitable candidates were selected if they lay well out of the Galactic plane. It is vital that faint targets are not obscured by background infra-red radiation from dust in the plane of the Galaxy. We therefore chose to observe NGC104 (47 Tuc), NGC5139 (ω Cen), NGC5272 (M3) and NGC7078 (M15) as they all have sufficiently high Galactic latitudes (see Table 1).

We expect the dust in a GC to be the result of mass loss from evolved stars within the cluster. Since the formation of dust in a stellar outflow is due to the condensation of elements of intermediate mass produced by the parent star, we would *a priori* expect a metal-rich GC to be more capable of dust production. Our targets range from relatively metal-rich to very metal-poor (see Table 1). Results may therefore identify the importance of metallicity on the production of dust in GCs.

Other conditions that favour these candidates include:

1. their large escape velocities, indicating that the GCs are more capable of retaining any circumstellar matter ejected into the intra-cluster medium (see Table 1).
2. The cores of all the clusters (except NGC5139) fit well inside the central pixel ($43.5'' \times 43.5''$) of each ISO map.
3. Odenkirchen et al. (1997) have calculated orbital parameters for three of the chosen clusters (no orbit is available for NGC5139) and found that they all passed through the plane of the Galaxy a few $\times\, 10^7$ years ago (see Table 1). Sufficient time has therefore passed for evolved stars within the GCs to have replenished their intra-cluster environments with circumstellar material.

With regard to the latter point, and following the method of Tayler & Wood (1975), we can use the results of Odenkirchen et al. to estimate the mass of dust we would expect to observe in each cluster by integrating the mass injection around the cluster orbit. Like Tayler & Wood, we assume that each star loses $0.2\,M_\odot$ of circumstellar material at the tip of the red giant branch and that the stars remain on the horizontal branch for

Table 1. Relevant globular cluster properties.

Target	[Fe/H][a]	Core radius[b] ($''$)	Half-light radius[b] ($''$)	Z-height[a] (kpc)	Galactic latitude[c] ($^\circ$)	Escape velocity[d] (km s^{-1})	Mass of cluster[e] (10^5 M$_\odot$)	Time since last plane crossing[f] (10^7 yrs)	Expected dust mass (10^{-2} M$_\odot$)
NGC104	–0.71	22.4	173.8	3.24	–45	56.8	13	6	23.4
NGC5139	–1.59	154.9	288.4	1.26	15	51.2	40	–	–
NGC5272	–1.66	30.2	67.6	10.00	79	34.3	6	14	4.2
NGC7078	–2.17	4.1	60.3	4.79	–27	40.9	20	4	0.2

[a] Djorgovski (1993), [b] Trager et al. (1993), [c] Djorgovski & Meylan (1993), [d] Webbink (1985), [e] Pryor & Meylan (1993), [f] Odenkirchen et al. (1997)

Table 2. Observational details.

Target	Date of observation	Camera	Total on-source integration time (s)	Integration time per pixel per wavelength (s)
NGC104	25 May 96	C100	2972	39.63
NGC104	09 Mar 98	C200	8766	365.25
NGC5139	17 Feb 97	C100	2970	39.60
NGC5272	10 Dec 96	C100	5446	72.61
NGC7078	01 Nov 96	C100	5446	72.61
NGC7078	26 Nov 96	C100	5446	72.61

1×10^8 years; we also use similar horizontal branch populations and apply a gas-to-dust ratio, scaled by metallicity assuming 100:1 by mass for solar metallicity, to determine expected dust masses (see Table 1). Expected dust masses for NGC104, NGC5272 and NGC7078 are given in Table 1.

3. Observations and reductions

We observed the four GCs with the PHT-C camera on board ISO (see Lemke et al. 1996, and Kessler et al. 1996, for descriptions of ISOPHOT and ISO respectively). The GCs NGC5139, NGC5272 and NGC7078 were observed in the 60 μm, 70 μm and 90 μm wavebands. NGC104 was observed at the same wavelengths and also in the 120 μm waveband on a separate date. Dates of observations and total on-source integration times are given in Table 2.

We obtained maps of the clusters at 60 μm, 70 μm and 90 μm using the C100 3 $\times$ 3 pixel array. NGC104 was observed at 120 μm with the C200 2 $\times$ 2 pixel array. Both cameras were used in raster mode, which is a sequence of staring observations on a 2-dimensional grid. For observations carried out by the C100 camera, there were 5 pointings per line, and the same number of lines in the whole pointing. The distance between adjacent pointings and lines was 135$''$. For observations carried out by the C200 camera, there were 8 pointings per line and 3 lines in the whole raster. The distance between adjacent pointings and lines was 180$''$. The total integration time per pixel, corresponding to each wavelength during an observation, is given in Table 2. Since a single pixel on the C100 camera was 43.5$''$ $\times$ 43.5$''$ in size, the raster parameters created a map which covered 675$''$ $\times$ 675$''$ of sky. A single pixel on the C200 camera was 89.4$''$ $\times$ 89.4$''$ in size, corresponding to a total sky coverage of 540$''$ $\times$ 1440$''$. The unvignetted field of view for the ISOPHOT instruments is 3$'$.

The data were reduced using PIA version 7.2.2(e) (see Gabriel et al. 1997) and calibrated using the internal radiation source FCS 1. The data were deglitched and the dark current was subtracted. A drift effect is a common feature in these data, arising from observations of targets, prior to current observations, that differ significantly in brightness. To minimise this effect, the internal radiation sources are initially calibrated by stars, planets and asteroids and are power tuned according to the observer's flux prediction. Thus, a signal is delivered similar to that expected from the target, and detector drifts caused by large flux steps are reduced. Despite this, we further corrected for drifting and the data were subsequently flatfielded using a median stack method described by B. Schulz (private communication).

Fig. 1 shows the observational results for NGC104 observed at 60, 70 and 90 μm. Similarly, Fig. 2 shows the observational results for NGC104 at 120 μm. All maps are in units of MJysr^{-1} and those obtained from the C100 camera have been smoothed by convolving with the 200 μm beam on the C200 camera. There is approximately a 10% relative uncertainty in each of the maps. The absolute and relative calibration accuracies per detector for extended sources are 20% and $<$30% respectively for the C100 camera in the 5–15MJysr^{-1} brightness range. These corresponding accuracies are the same for the C200 camera in the 3–10MJysr^{-1} brightness range (Klaas et al. 1998).

Since pixels on the edge of the maps lie well outside the respective half-light radius of each cluster (see Table 1), we assumed that the flux in the faintest pixels was a good indication of the flat background flux levels. These values have therefore been subtracted from the data and the discussion hereafter refers to background subtracted data. Table 3 gives the observed surface brightnesses in the core for each cluster. The high surface brightnesses seen in the direction of NGC5139 occur since the core of this cluster is large relative to the size of the beam, and results have therefore been scaled to allow for this.

We have compared IRAS results for NGC104, described by Gillett et al. (1988) and by Origlia et al. (1996), with our own, and results are given in Table 4. We have converted surface brightnesses in the central pixel of the ISO maps into fluxes,

Table 3. Observed surface brightness in the core of each cluster in MJysr^{-1}.

Wavelength (μm)	NGC104	NGC5139	NGC5272	NGC7078
60	4.42 $\pm$1.42	84.65 $\pm$56.88	2.26 $\pm$2.08	3.33 $\pm$1.89
70	2.84 $\pm$1.27	94.66 $\pm$70.62	4.96 $\pm$2.12	2.65 $\pm$1.95
90	2.51 $\pm$1.04	73.25 $\pm$74.60	1.23 $\pm$1.42	3.14 $\pm$1.80
120	0.67 $\pm$0.39	–	–	–

Table 4. Comparison of results from this paper with IRAS observational results for NGC104.

Facility	Wavelength (μm)	Flux (Jy)	Size of beam	Reference
IRAS	12	8.10 $\pm$0.80	6′	(a)
	25	2.50 $\pm$0.20		
	60	0.32 $\pm$0.04		
	100	0.20 $\pm$0.06		
IRAS	12	11.00	2′	(b)
	25	3.00		
ISO	60	0.20 $\pm$0.06	43.5″	(c)
	70	0.13 $\pm$0.05		
	90	0.11 $\pm$0.05		
	120	0.03 $\pm$0.02		

(a) Gillett et al. (1988), (b) Origlia et al. (1996), (c) This paper.

by assuming that the emission is distributed evenly throughout this pixel. Since one pixel is well matched in size to the core of this cluster, this is a reasonable assumption. Our results are in reasonable agreement with both Gillett et al. (1988) at 60 μm and 100 μm, and Origlia et al. (1996), if we extrapolate along the Rayleigh Jeans tail to 60 μm and longer wavelengths. This is only valid if the emission in NGC104 is strongly concentrated within the core of the cluster. Since the stellar density gradients in GCs show that the cores are extremely dense, there is a strong possibility that this will be the case.

We do not confidently identify any point sources in the NGC104 data corresponding a) to those identified in the IRAS data by Gillett et al. (1988), b) in the IRAS point source catalogue and c) in the data by Jorissen et al. (1999).

4. Results

Gillett et al. (1988) detected an infrared excess at 100 μm in NGC104 with IRAS, which they attributed to dust. In the 60 μm waveband they found that the cluster emitted radiation consistent with that expected of the stars within. We have therefore used two methods to determine possible IR excesses from the ISO data.

In the first method, we assume that the 60 μm ISO emission from our four observed clusters is entirely stellar. We then extrapolate to 70, 90 and 120 μm where relevant, to find the expected stellar emission at these wavelengths. We subtract these values from the results obtained from the data and look for possible IR excesses at these wavelengths.

In the second method, we fit models to observational optical surface brightness profiles (Da Costa & Freeman, 1976, for NGC5272; Da Costa, 1979, for NGC104 and NGC5139; Chun et al., 1980, for NGC7078). Such profiles are fit best when a stellar density law given by the RPKK model (Richstone & Tremaine, 1986)

$$\rho(r) = \frac{\rho_0}{\left(1 + \left(\frac{r}{r_c}\right)^2\right)^{3/2}}$$

is assumed, where $\rho(r)$ corresponds to the stellar surface density at position r, and ρ_0 is the constant surface density within the core (radius r_c), of the cluster. Parameters such as luminosity, radius and mass corresponding to metal-poor stars are obtained from models given by Mazzitelli et al. (1995; and private communication), D'Antona & Mazzitelli (1996; and private communication), Caloi et al. (1997) and Jimenez & MacDonald (1996; and private communication). We extrapolate our models to 60, 70, 90 and 120 μm, convolving them through the appropriate ISO filter (Klaas et al. 1994) and again, compare computed fluxes with the data, to look for possible IR excesses in any of the relevant wavebands.

Since we are searching for grains that have been ejected directly into the intra-cluster medium, we presume they would have properties associated with circumstellar grains rather than interstellar grains, which have undergone processing. We therefore assume any grains to be either silicate or amorphous carbon in type.

If we observed silicate and amorphous carbon grains in the cores of all of the four observed clusters we would expect the dust temperatures to be $\sim$ 40 K and 70 K respectively (Angeletti et al. 1982). These temperatures correspond to wavelengths of maximum emission of $\sim$ 60 μm and 35 μm respectively, assuming a β-index of unity. With respect to the second method, it is therefore reasonable to assume that, if we found evidence of dust in any of the four clusters at 70, 90 or 120 μm, we would also see it at 60 μm, unless the dust is unrealistically cold.

Using both methods, we find that none of the four clusters show an infra-red excess at 60, 70 or 90 μm. Furthermore, NGC104 does not show an infra-red excess at 120 μm. We therefore place 3σ upper limits on the excess surface brightness and mass of dust present in the cores of each cluster using optical data from Martin & Rogers (1987; carbon) and Suh (1991; silicates). We calculate dust masses at equilibrium dust temperatures of 100 K and 150 K, as well as 40 K and 70 K, the latter two being typical of expected intra-cluster dust temperatures in GCs (Angeletti et al. 1982). We take the grain densities of amorphous carbon and silicate dust to be ρ = 2000 kgm^{-3} and 3300 kgm^{-3} respectively; we again assume a β-index of unity. Our results are given in Table 5. NGC7078 was observed twice and results from both datasets are consistent.

5. Discussion

Gillett et al. (1988) claimed to have detected 3×10^{-4} M$_\odot$ of silicate dust in the central 6′ of 47 Tuc. Our observations of 47

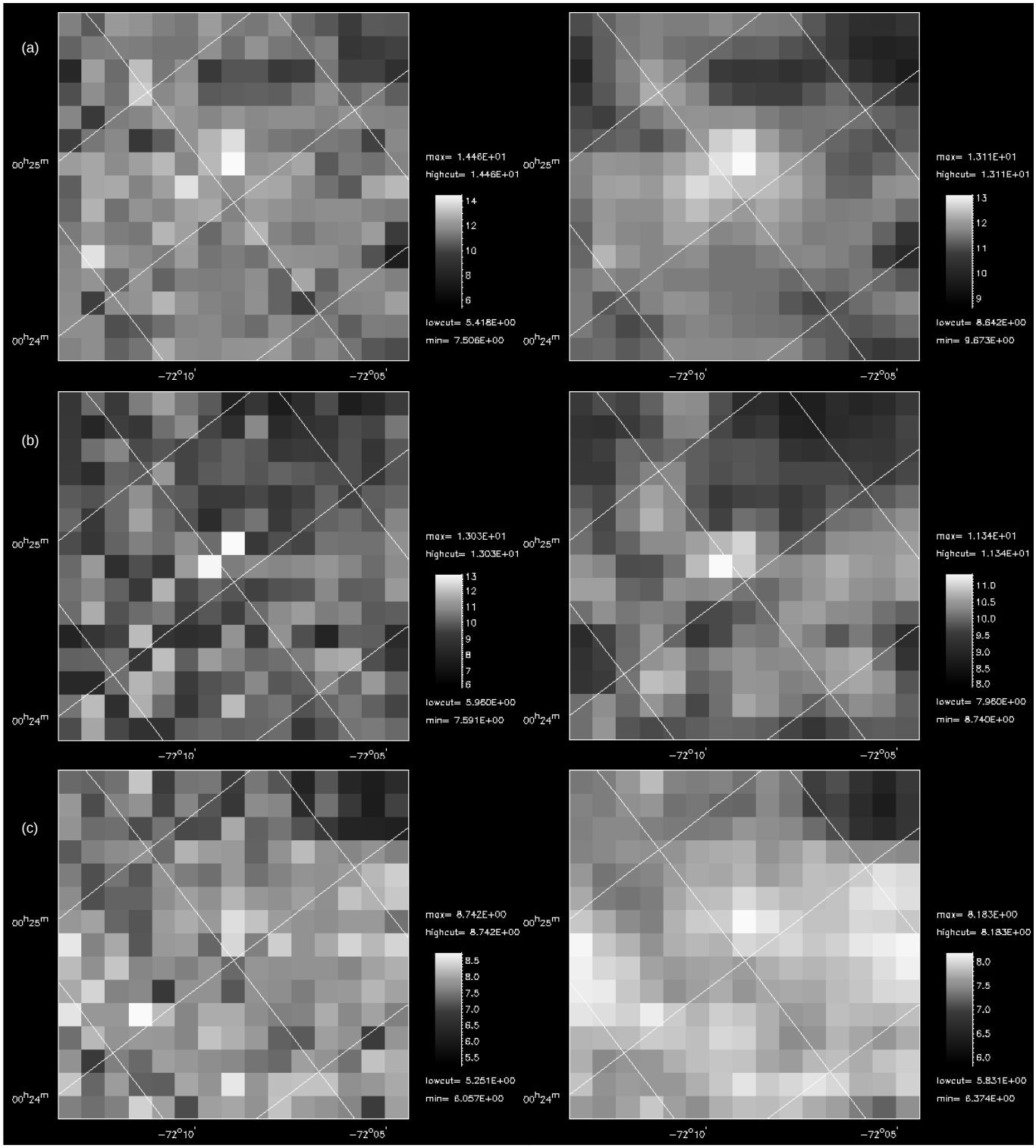

Fig. 1a–c. Observational results for NGC104 at **a** 60 μm, **b** 70 μm and **c** 90 μm. For each wavelength the figure on the right is the map convolved with the 200 μm beam on the C200 camera. The units are in MJysr^{-1}.

Tuc do not confirm this result. We find a 3σ upper limit on the mass of dust in this cluster to be between 1.7...1.8 $\times$ 10^{-4} M$_{\odot}$ for silicate grains at the temperature assumed by Gillett et al.

The results we obtained for NGC104, NGC5139 and NGC5272 confirm that GCs are lacking in intra-cluster material, since our upper limits are much lower then the expected dust masses (see Table 1). If the dust in NGC7078 has an equi-

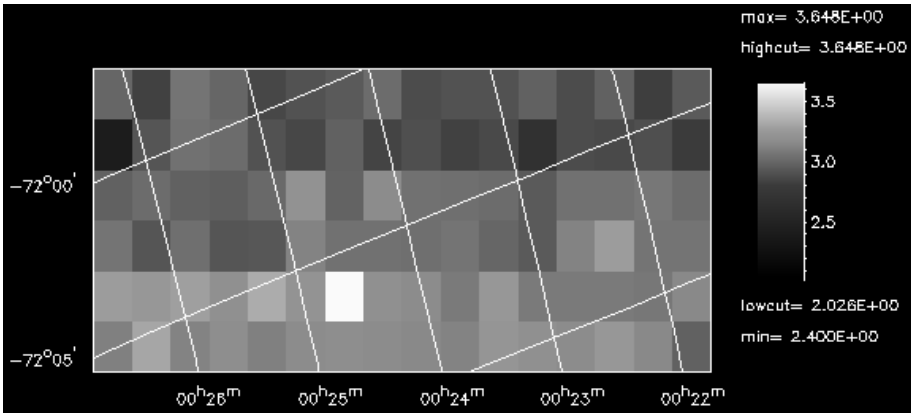

Fig. 2. Observational results for NGC104 at 120 μm. The units are in MJysr^{-1}.

Table 5. 3σ upper limits on the excess surface brightness and dust masses.

Target	Surface Brightness (M Jy sr^{-1})		SILICATES T_{dust} (K)	SILICATES M_{dust} ($M_\odot$)		AMORPHOUS CARBON T_{dust} (K)	AMORPHOUS CARBON M_{dust} ($M_\odot$)	
	method one	method two		method one	method two		method one	method two
NGC104	4.9[b]	1.7[d]	40	5.7 10^{-4}	1.8 10^{-4}	40	3.5 10^{-4}	1.1 10^{-4}
			70	5.8 10^{-5}	4.3 10^{-5}	70	3.5 10^{-5}	2.6 10^{-5}
			100	2.2 10^{-5}	2.2 10^{-5}	100	1.3 10^{-5}	1.3 10^{-5}
			150	9.4 10^{-6}	1.1 10^{-5}	150	5.7 10^{-6}	7.0 10^{-6}
NGC5139	278.5[b]	254.6[a]	40	3.6 10^{-2}	4.4 10^{-2}	40	2.1 10^{-2}	2.5 10^{-2}
			70	3.7 10^{-3}	3.0 10^{-3}	70	2.2 10^{-3}	1.8 10^{-3}
			100	1.4 10^{-3}	9.9 10^{-4}	100	8.4 10^{-4}	6.0 10^{-4}
			150	6.0 10^{-4}	3.9 10^{-4}	150	3.5 10^{-4}	2.3 10^{-4}
NGC5272	5.3[c]	8.4[a]	40	2.6 10^{-3}	6.2 10^{-3}	40	1.5 10^{-3}	3.8 10^{-3}
			70	4.1 10^{-4}	4.4 10^{-4}	70	2.4 10^{-4}	2.7 10^{-4}
			100	1.8 10^{-4}	1.4 10^{-4}	100	1.1 10^{-4}	8.7 10^{-5}
			150	8.7 10^{-5}	5.7 10^{-5}	150	5.3 10^{-5}	3.5 10^{-5}
NGC7078	7.4[b]	6.5[a]	40	4.4 10^{-3}	5.1 10^{-3}	40	2.7 10^{-3}	3.1 10^{-3}
			70	4.5 10^{-4}	3.6 10^{-4}	70	2.8 10^{-4}	2.2 10^{-4}
			100	1.7 10^{-4}	1.2 10^{-4}	100	1.0 10^{-4}	7.3 10^{-5}
			150	7.3 10^{-5}	4.7 10^{-5}	150	4.4 10^{-5}	2.8 10^{-5}

[a] 60 μm data, [b] 70 μm data, [c] 90 μm data, [d] 120 μm data.

librium temperature of 70 K or above, then this cluster is also deficient in such material. If however the dust has an equilibrium temperature of 40 K, then our data do not allow us to draw any conclusions.

HEPE have discussed the efficiency of grain sputtering for the case of NGC6356. For the GCs considered here, we use the orbits of Odenkirchen et al. (1997) and the method of Nordgren et al. (1992) to find the variation of electron density in the halo as NGC104, NGC5272 and NGC7078 move along their respective paths. Assuming that, since the last plane crossing, equal fractions of grains have been injected into the intra-cluster medium at a steady state, and using the expected dust masses and times since the last plane crossings (Table 1), we can calculate the residual dust mass in each cluster after grain erosion has occured. We take a grain radius of 0.1 μm before sputtering.

We find the initial mass of dust is reduced by only $\sim 1\%$ throughout each GC orbit. Grain erosion is again therefore ineffective since each cluster climbs high out of the galactic plane on a relatively short timescale. Sputtering by halo gas can not therefore be the removal mechanism at work within these three clusters, supporting the conclusion of HEPE.

Since we have new upper limits on the mass of dust in four GCs, Fig. 3 illustrates how dust mass varies with three cluster properties: metallicity, escape velocity and Z-height. We have also included the firm detection of dust in NGC6356 (HEPE) and the claimed detection in NGC104 (Gillett et al. 1988) for comparison.

Although we cannot rely on upper limits to constrain possible relationships between observed dust masses and cluster parameters, we can at least use the detection by HEPE, and the

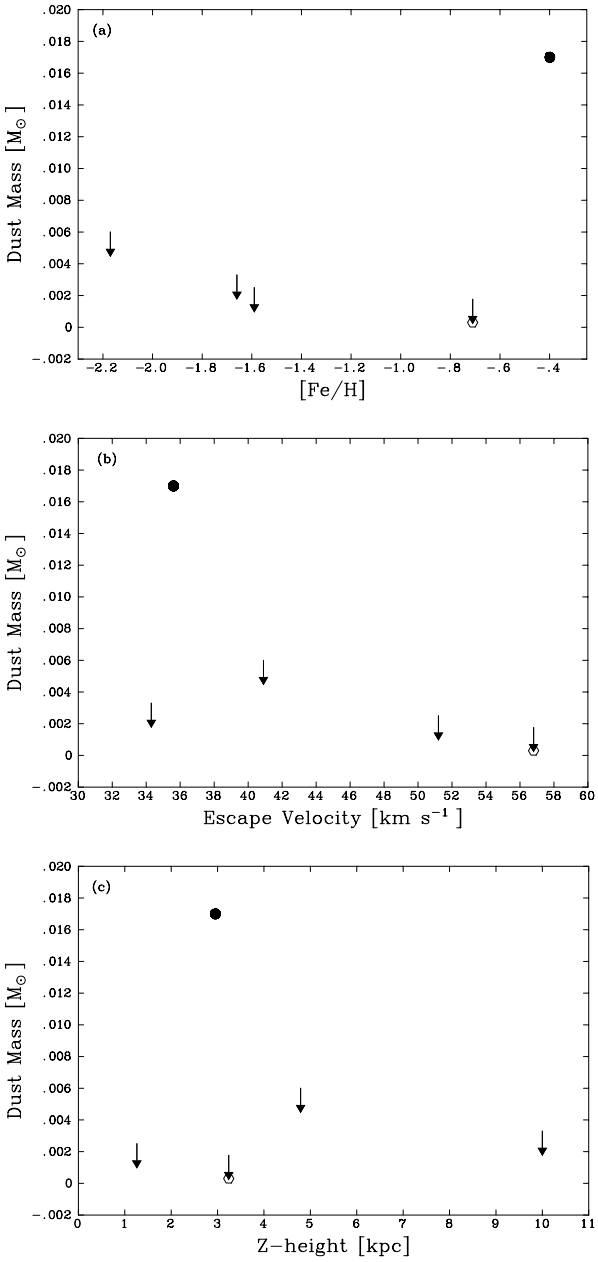

Fig. 3a–c. Mass of GC dust versus three cluster properties; **a** metallicity of cluster, **b** escape velocity of cluster, **c** Z-height of cluster. In each case the arrows correspond to ISO upper limits, the filled circle corresponds to the sub-millimetre detection of dust in NGC6356 (HEPE) and the open hexagon corresponds to the claimed IRAS detection in NGC104 (Gillett et al. 1988).

claimed detection by Gillett et al. (1988) to look for pointers to such relationships. The detection of dust in NGC6356 suggests that metallicity is more likely to be a factor than either escape velocity or Z-height in determining dust content. This reinforces the conclusions of Jacoby et al. (1997) and Buell et al. (1997), who found that the planetary nebula in NGC7078 is metal-deficient, implying that the metallicity of evolved stars in this cluster mirrors the metallicity of the cluster.

We would expect GCs with high escape velocities to retain more dust than those with low escape velocities. However, Fig. 3b suggests that this is not consistent with the data and upper limits we have to date. Since the orbital parameters of NGC6356 are not available, it is difficult to comment on the relationship between Z-height and dust content. However, dust removal mechanisms have been proposed which depend directly on the clusters position in the Galactic halo. Since NGC6356 and NGC104 lie at similar Z-heights, Fig. 3c suggests that Z-height may not be an important factor in determining the dust content of a GC.

6. Conclusions

We have presented ISO observations of GCs and reported new upper limits on the masses of dust. Our limits support previous conclusions that GCs are deficient in intra-cluster dust grains, although in the case of NGC7078, if the dust has an equilibrium temperature of 40 K, no conclusion can be drawn. We again find that sputtering of dust grains by halo gas is unlikely to be significant within NGC104, NGC5272 and NGC7078. We must therefore conclude that the formation of dust is inhibited, or that some other mechanism is at work to remove any dust from the cluster on a short timescale. With regard to the former, our results confirm that the metallicity of the cluster may be an influencing factor.

Acknowledgements. We acknowledge the help of Drs Phil Richards, Carlos Gabriel, Bernhard Schulz and Rene Laureijs. We also acknowledge Drs Francesca D'Antona, Italo Mazzitelli, Vittoria Caloi and Raul Jimenez. We thank Dr Gillian Knapp for helpful comments. The ISOPHOT data presented in this paper were reduced using PIA, which is a joint development by the ESA Astrophysics Division and the ISOPHOT Consortium. MELH is supported by a UK Particle Physics and Astronomy Research Council (PPARC) studentship, SPSE by a PPARC research assistantship.

References

Angeletti L., Blanco A., Bussoletti E., et al., 1982, MNRAS 199, 441
Bergbusch P.A., VandenBerg D.A., 1992, ApJS 81, 163
Buell J.F., Henry R.B.C., Baron E., Kwitter K.B., 1997, ApJ 483, 837
Caloi V., D'Antona V., Mazzitelli I., 1997, A&A 320, 823
Chun M.S., Suh Y.R., Lee Y.B., 1980, JKAS 13, 27
D'Antona F., Mazzitelli I., 1996, ApJ 456, 329
Da Costa G.S., Freeman K.C., 1976, ApJ 206, 128
Da Costa G.S., 1979, AJ 84, 505
Djorgovski S., Meylan G., 1993, In: Djorgovski S.G., Meylan G. (eds.) Structure and Dynamics of Globular Clusters. ASP Conference Series Vol. 50, p. 325
Djorgovski S., 1993, In: Djorgovski S.G., Meylan G. (eds.) Structure and Dynamics of Globular Clusters. ASP Conference Series Vol. 50, p. 373
Gabriel C., Acosta-Pulido J., Heinrichsen I., et al., 1997, In: Hunt G., Payne H.E. (eds.) Proc. of the ADASS VI conference, ASP Conf. Ser. Vol. 125, p. 108
Gillett F.C., de Jong T., Neugebauer G., Rice W.L., Emerson J.P., 1988, AJ 96, 116

Hopwood M.E.L., Evans A., Penny A., Eyres S.P.S., 1998, MNRAS 301, L30 (HEPE)
IRAS, 1988, IRAS point source catalogue. Aumann H., et al. (eds.) NASA RP-1190
Jacoby G.H., Morse J.A., Fullton L.K., Kwitter K.B., Henry R.B.C., 1997, AJ 114, 2611
Jimenez R., MacDonald J., 1996, MNRAS 283, 721
Jorissen A., Coheur P.F., Alvarez R., Groenewegen M.A.T., 1999, In: Cox P., Kessler M.F., (eds.) The Universe as seen by ISO. ESA-SP 427, p. 341
Kessler M.F., Steinz J.A., Anderegg M.E., et al., 1996, A&A 315, L27
Klaas U., Krüger H., Heinrichsen I., Heske A., Laureijs R.J., 1994, ISO observer's manual V3.1
Klaas U., Laureijs R.J., Radovich M., Schulz B., 1998, ISOPHOT calibration accuracies V2.0
Knapp G.R., Gunn J.E., Connolly A.J., 1995, ApJ 448, 195
Lemke D., Klaas U., Abolins J., et al., 1996, A&A 315, L64
Martin P.G., Rogers C., 1987, ApJ 322, 374
Mazzitelli I., D'Antona F., Caloi V., 1995, A&A 302, 382
Nordgren T.E., Cordes J.M., Terzian Y., 1992, AJ 104, 1465
Odenkirchen M., Brosche P., Geffert M., Tucholke H.J., 1997, New Astronomy 2, 477
Origlia L., Ferraro F.R., Fusi Pecci F., 1996, MNRAS 280, 572
Penny A.J., Evans A., Odenkirchen M., 1997, A&A 317, 694
Pryor C.& Meylan G., 1993, In: Djorgovski S.G., Meylan G. (eds.) Structure and Dynamics of Globular Clusters. ASP Conference Series Vol. 50, p. 357
Richer H.B., Fahlman G.G., Ibata R.A., et al., 1995, ApJ 451, L17
Richstone D.O., Tremaine S., 1986, AJ 92, 72
Suh K-W., 1991, Ap&SS 181, 237
Tayler R.J., Wood P.R., 1975, MNRAS 171, 467
Trager S.C., Djorgovski S., King I.R., 1993, In: Djorgovski S.G., Meylan G. (eds.) Structure and Dynamics of Globular Clusters. ASP Conference Series Vol. 50, p. 347
Webbink R.F., 1985, In: Goodman J. (ed.) Proc IAU Symp. 113, Reidel, Dordrecht, p. 541